Low frequency of intracranial progression in advanced NSCLC patients treated with cancer immunotherapies

Short Title: Cancer immunotherapy and intracranial progression

Authors: Naoya Kemmotsu, Kiichiro Ninomiya, Kei Kunimasa, Takamasa Ishino, Joji Nagasaki, Yoshihiro Otani, Hiroyuki Michiue, Eiki Ichihara, Kadoaki Ohashi, Takako Inoue, Motohiro Tamiya, Kazuko Sakai, Youki Ueda, Hiromichi Dansako, Kazuto Nishio, Katsuyuki Kiura, Isao Date, and Yosuke Togashi

Table of contents

Supplementary Figure S1. Gadolinium-enhanced brain magnetic resonance image (MRI)

Supplementary Figure S2. Additional analyses for PFS and OS

Supplementary Figure S3. *In vivo* efficacy of PD-1 blockade against MC-38 tumors

Supplementary Figure S4. TIL analyses in subcutaneous LL/2-OVA tumors

Supplementary Figure S5. Rechallenges with the same MC-38 tumor cells in mice treated with PD-1 blockade

Supplementary Table S1. Patient characteristics

Supplementary Table S2. Summary of antibodies used in flow cytometry analyses

Supplementary Figure S1. Gadolinium-enhanced brain magnetic resonance image (MRI)

Sixty-eight-year-old male patient with non-squamous NSCLC underwent pembrolizumab as first-line chemotherapy. This patient received radiotherapy two weeks before the treatment.

Supplementary Figure S2. Additional analyses for PFS and OS

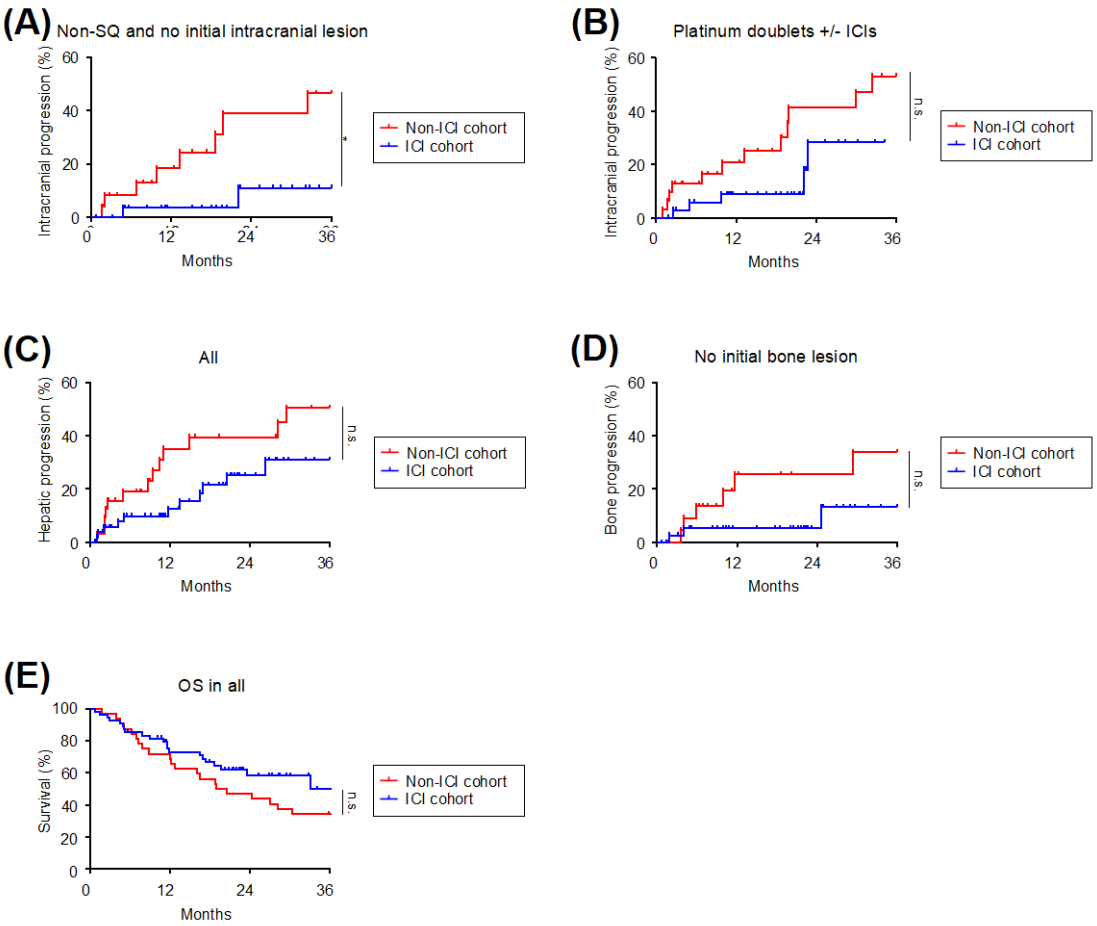

Patients who received standard platinum-doublet chemotherapies (N = 32) or PD-1 blockade therapies without anti-CTLA-4 mAb (N = 54) as first-line therapies were enrolled in this study as the non-ICI and ICI cohorts, respectively. OS, intracranial, hepatic, and bone progression-free survival (PFS) were defined as the time from the initiation of first-line standard chemotherapy to death from any cause, the time from the initiation of first-line standard chemotherapy to the first observation of intracranial disease progression or death from any cause, the time from the initiation of first-line standard chemotherapy to the first observation of hepatic disease progression or death from any cause, and the time from the initiation of first-line standard chemotherapy to the first observation of bone disease progression or death from any cause, respectively. Intracranial PFS curves for patients with non-SQ without initial intracranial lesions and patients received platinum doublet +/- ICI therapies are shown in **(A)** and **(B)**, respectively. Hepatic PFS curves for all patients and bone PFS curves for patients without initial bone lesions are shown in **(C)** and **(D)**, respectively. OS of all patients is shown in **(E)**.

PFS and OS was analyzed using the Kaplan–Meier method and compared among groups using the log-rank test. *, $P < 0.05$; n.s., not significant.

Supplementary Figure S3. *In vivo* efficacy of PD-1 blockade against MC-38 tumors

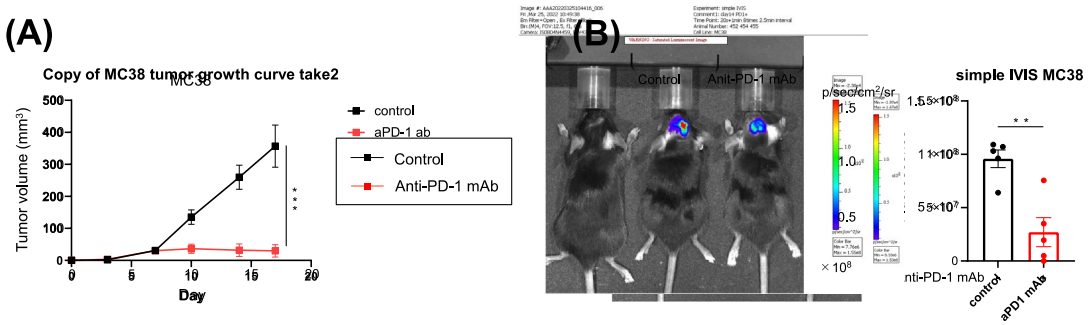

(A) *In vivo* efficacy of PD-1 blockade against subcutaneous MC-38 tumors. Mouse experiments were performed as described in **Figure 2A**.
(B) *In vivo* efficacy of PD-1 blockade against intracranial MC-38 tumors. Mouse experiments were performed as described in **Figure 2B**, and IVIS was used for imaging intracranial tumors on Day 14. Representative imaging and the summary are shown.

All *in vivo* experiments were performed in duplicate, with similar results. Two-way ANOVA was used in (A), and a t test was used in (B) for statistical analyses. The means and SEMs are shown. **, $P < 0.01$; ***, $P < 0.001$.

Supplementary Figure S4. TIL analyses in subcutaneous LL/2-OVA tumors

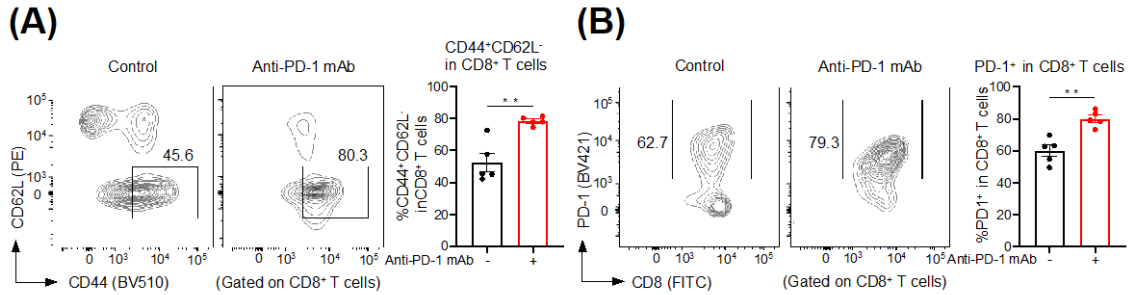

The proportions of $CD44^{+}CD62L^{-}CD8^{+}$ T cells (A) and $PD\text{-}1^{+}CD8^{+}$ T cells (B) in subcutaneous LL/2-OVA tumors. Mouse experiments were performed as described in **Figure 2A**, and tumors were harvested on Day 14 for evaluation by flow cytometry (n = 5 per group). Representative flow cytometry staining (left) and summaries (right) are shown.

All *in vivo* experiments were performed in duplicate, with similar results. T tests were used for statistical analyses. The means and SEMs are shown. **, $P < 0.01$.

Supplementary Figure S5. Rechallenges with the same MC-38 tumor cells in mice treated with PD-1 blockade

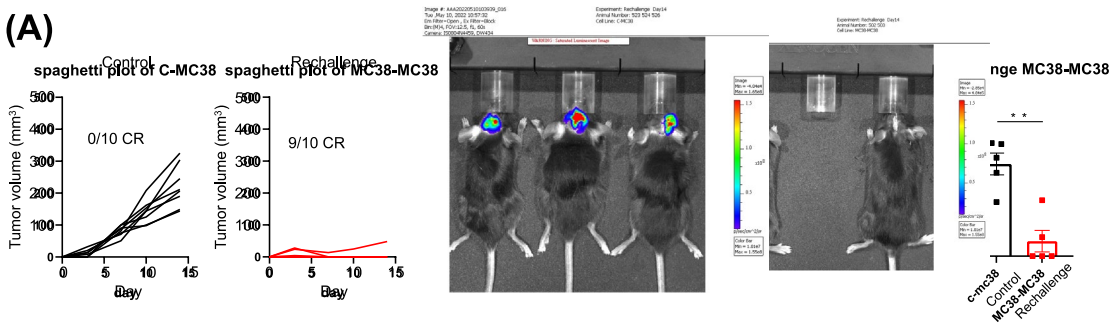

(A) Volume of each rechallenged MC-38 tumor. Mice that had completely eradicated the initial subcutaneous tumors after anti–PD-1 mAb were subcutaneously rechallenged with the same tumor cells on Day 32 (n = 10 per group). The means of the long and short diameters were used to generate tumor growth curves, and the volume of each tumor is shown. CR, complete rejection.
(B) Intracranial rechallenge of MC-38/Luc tumor growth. Mice that had completely eradicated the initial subcutaneous tumors after anti–PD-1 mAb were intracranially rechallenged with the same tumor cells on Day 32 (n = 5 per group). IVIS was used for imaging intracranial tumors on Day 46. Representative imaging and the summary are shown.

All *in vivo* experiments were performed in duplicate, with similar results. A t test was used in (B) for statistical analysis. The means and SEMs are shown. **, $P < 0.01$.

Supplementary Table S1. Patient characteristics

Features	**Non-ICI cohort (n = 32)**	**ICI cohort (n = 54)**	***P***
Age, years [median] (range)	62 (48–73)	68.5 (46–94)	0.011
Sex (male/female)	26/6	44/10	0.978
Performance status (0/1 or 2)	32/0	50/4	0.114
Histology (SQ/non-SQ)	1/31	17/37	0.001
Initial intracranial lesions (yes/no)	6/26	8/46	0.632
Initial hepatic lesions (yes/no)	3/29	4/50	0.747
Initial bone lesions (yes/no)	9/23	14/40	0.823
First line therapy (Platinum doublet/PD-1 blockade alone/PD-1 blockade + platinum)	32/0/0	0/18/36	-

ICI, immune checkpoint inhibitor; SQ, squamous cell carcinoma; CNS, central nervous system.

Supplementary Table S2. Summary of antibodies used in flow cytometry analyses

Molecule	Tag	Clone	Company
CD3	Alexa Fluor 700	500A2	BD bioscience
CD4	PerCP-Cy5.5	RM4-5	BD bioscience
CD8a	FITC	53-6.7	BD bioscience
CD44	BV510	IM7	BD bioscience
CD62L	PE	MEL-14	BD bioscience
CD127	PE-CF594	SB/199	BD bioscience
KLRG1	PE-Cy7	2F1	eBioscience
CD279	BV421	J43	BD bioscience
H-2K^{b}-SIINFEKL	APC	-	Immudex
Fixable Viability Dye	APC-Cy7	-	eBioscience